Modeling for Detonation and Energy Release from Peroxides and Non-Ideal Improvised Explosives

Matthew Anthony PRICE and Ang How GHEE

Energetics Research Institute,
Nanyang Technological University, Singapore
E-mail: mattprice@ntu.edu.sg; hgang@ntu.edu.sg

Abstract: This work focuses on the development of models for predicting explosive power and air blast from the detonation of organic peroxides (TATP and HMTD) and non-ideal explosives involving ammonium nitrate, urea nitrate, and chlorates. CHEETAH calculations assuming ideal behaviour are in agreement with literature data for peroxides. However, the detonation behaviour of non-ideal explosives is dependent on charge size and confinement. This behaviour is investigated using thermo-chemical calculations with Kinetic CHEETAH, and reactive flow models with AUTODYN. A simplified ignition and growth (I&G) model was calibrated using experimental charge diameter vs. VoD data. I&G models are used to predict the front curvature, reaction zone structure, and energy release from the non-ideal explosives. Detonation and air blast predictions for peroxides and unconfined and confined (paper, plastic, steel) non-ideal charges are presented.

Keywords: improvised explosive, non-ideal, reactive flow, ANFO, peroxide

Introduction

An understanding of improvised explosive materials (IEM) is vital for combating the growing terrorism threat. Recent terrorist attacks in the UK and Middle East have shown an increased usage of peroxides such as TATP and HMTD, while larger IED often use non-ideal explosives such as ANFO. To evaluate the threat from these two groups of IEM, we use CHEETAH 2.0 and ANSYS AUTODYN v.11 to predict detonation velocity and explosive power (via detonation energy and air blast).

Calculations for TATP and HMTD assume ideal behaviour, while ANFO, AN emulsion, and urea nitrate (UN) require non-ideal detonation theory and reactive flow models to investigate the effects of charge size and confinement. Models for a potassium chlorate and paraffin (PC/Paraffin 90:10) mixture demonstrate that the methodology can be extended to an explosive with little experimental data available.

Theory

Ideal Detonation

Chapman-Jouguet (CJ) detonation theory predicts the ideal detonation condition for explosives by assuming a zero-thickness reaction zone with an instantaneous jump to detonation products in thermodynamic equilibrium. Thermo-chemical codes, such as CHEETAH, accomplish this by using a library containing product species with thermodynamic and equation of state data. A "standard run" in CHEETAH 2.0 is used to calculate the CJ state, detonation product species, and the adiabatic expansion which is fit to the JWL equation of state (EOS) [1]:

$$P = Ae^{-R_1V} + Be^{-R_2V} + CV^{-(1+\omega)}, \tag{1}$$

where A, B, C, R_1, R_2, and ω are fitted parameters and V is the reduced volume,

$$V = \frac{\upsilon}{\upsilon_0} = \frac{\rho_0}{\rho}. \tag{2}$$

Non-Ideal Detonation

The reactive flow models use a simplified Ignition and Growth (I&G) model that is calibrated to experimental data following the method by Souers *et al*. for JWL++ [2]. The Lee-Tarver I&G model in AUTODYN is used with the JWL EOS to control the reaction rate of the explosive material given by:

$$\frac{\partial F}{\partial t} = I(1-F)^b(\mu - a)^x + G_1(1-F)^c F^d P^y + G_2(1-F)^e F^g P^z. \tag{3}$$

F is the reaction ratio (ratio of the detonation products mass to total explosive mass), P is the pressure, and I, b, a, x, G_1, c, d, y, G_2, e, g, and z are constants for the ignition term and two growth terms. The compression, μ, is defined as:

$$\mu = \rho\Big/\rho_0 - 1. \tag{4}$$

The ignition behaviour is not of interest and was found to have a minimal influence on the steady state solution. Contribution of the ignition term is limited to $F_{max} = 0.02$, with a constant set of ignition parameters assumed from common values for other explosives ($I = 40 \ \mu s^{-1}$, $b = 0.222$, $a = 0$, $x = 4$). The second growth term (G_2) is excluded and the remaining growth term is reduced to:

$$\frac{\partial F}{\partial t} = G(1 - F)P^b. \tag{5}$$

G is the rate constant with units ($\mu s^{-1} GPa^{-b}$) and the pressure exponent has been changed to 'b' for consistency with literature [2]. Lee-Tarver I&G in AUTODYN maintains pressure equilibrium, but not thermal equilibrium, between the reacted and unreacted explosive. The unreacted explosive is modelled with a Mie-Grüneisen form of the Linear (U_s-u_p) EOS,

$$P = P_H + \frac{\Gamma_0 \rho_0}{V}\left(e - \frac{1}{2}\frac{P_H}{\rho_0}(1 - V)\right), \text{ where } P_H = \frac{\rho_0 C_0^2 (1 - V)}{[1 - s(1 - V)]^2}. \tag{6}$$

Non-ideal explosives are modelled in Kinetic CHEETAH (K-CHEETAH) using Wood-Kirkwood detonation theory [1] to predict the timescale of the reaction kinetics and expansion. The theory uses a one-dimensional solution with energy flow away from the axis approximated from the radial expansion or radius of curvature. The K-CHEETAH calculations also use a simple pressure-dependent reaction rate which reduces to eq. 5. Both the K-CHEETAH and I&G models are used to study steady detonation in cylindrical charges.

Detonation Energy (Ideal and Non-Ideal)

Explosive power for producing air blast, driving fragments, etc. can be predicted by different methods. One simple method is the thermodynamic heat of detonation which is found from the heats of formation, ΔH_f^0, for the detonation products and explosive reactants via

$$\Delta H_d^0 = -\left\{\sum n \cdot \Delta H_f^0 (\text{products}) - \sum n \cdot \Delta H_f^0 (\text{reactants})\right\}. \tag{7}$$

Alternatively, the hydrodynamic expansion work can be found by eq. 8 as the pressure-volume work from the CJ point less the shock compression energy (E_c):

$$E_{\det} = W = \int_{V_{cj}}^{V} PdV - E_c \text{ , where } E_c = \frac{1}{2}(P_{CJ})(1 - V_{CJ}). \tag{8}$$

The detonation energy from the AUTODYN models is calculated with eq. 9, where E_0 is the initial explosive internal energy of the explosive and E_{INT} is the internal energy calculated by the code.

$$E_{\det} = E_0 - E_{INT}. \tag{9}$$

Equations 7 and 8 give approximately the same result after expansion to standard atmosphere, but the hydrodynamic method is preferred because it allows for calculation of the detonation energy with expansion. Air blast energy is expressed as an equivalence to TNT (*TNTeq*) on a per-weight basis. This can be directly calculated from measured blast pressure or impulse, or predicted from a ratio of E_{det} for the explosive of interest to TNT.

The energy output from non-ideal explosives is dependent on charge size which makes it difficult to define for traditional modelling methods (i.e. JWL with Program Burn). For example, the ANFO EOS in the AUTODYN material library has a notably lower detonation energy ($E_0 \approx 2.5$ kJ/cc) than CHEETAH calculations ($E_0 \approx 3.5$ kJ/cc) and other experiments ($E_0 \approx 3.2$ kJ/cc) [3]. It was proposed that the diameter of the cylinder test used for this EOS was not large enough to overcome the non-ideal effects [3, 4].

TATP and HMTD (Peroxides)

Detonation Velocity

CHEETAH calculations using the NEWC1 product library gave the best fit to the experimental detonation velocity-density curves for TATP and HMTD [5, 6]. Calculations were performed using the entire product library (default) and limited product sets based on recent literature for these peroxides. Dubnikova *et al.* [7] predicted the decomposition of TATP using density functional theory (DFT) into C_3H_6O, CO_2, C_2H_6, and O_2. Hiyoshi *et al.* [8] measured the decomposition products of TATP and HMTD using a T-Jump/FTIR method. The T-Jump experiments heated the compounds at a rate of 2000 K/s in Argon which is more analogous to the detonation reaction timescale than traditional thermal analysis. The effect of limiting the product species on the calculated detonation velocity is shown in Figure 1.
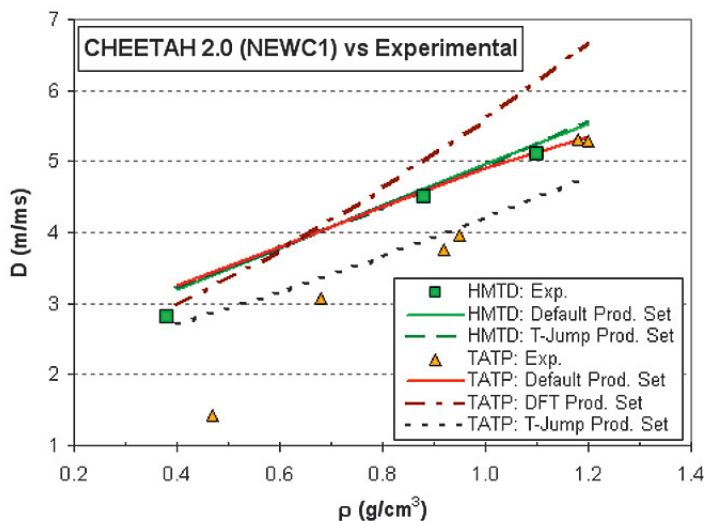
Figure 1. Experimental and CHEETAH 2.0 calculated detonation velocities using default and limited product sets for TATP and HMTD.

Table 1. Comparison of decomposition product concentrations (mol %) from T-Jump experiments and CHEETAH calculations at ~50% ρ_{TMD}

TATP			HMTD		
ρ_0 (g/cm³) =	0.6		ρ_0 (g/cm³) =	0.8	
ρ_{TMD} (g/cm³) =	1.22 [9]		ρ_{TMD} (g/cm³) =	1.57 [10]	
Product Species	T-Jump Exp.	CHEETAH	Product Species	T-Jump Exp.	CHEETAH
CH_4	46	39	CO	78	23
CO_2	28	36	HCN	11	12
C_2H_4	14	16	CHNO	3	9
C_2H_2O	5	6	CH_4	3	20
H_2O	2	2	CO_2	1	12
C_3H_6O	2	~0	NH_3	1	4
$C_3H_6O_2$	2	~0	CH_2O	1	~0
CH_2O	1	~0	H_2O	1	20

CHEETAH calculated detonation velocities for HMTD agree well with experiments using either the default product library or T-Jump product set. For TATP, the default library only agrees near maximum density (ρ_{TMD}), but the

T-Jump products give a better agreement near the bulk density (0.6-0.8 g/cm³). Using the DFT product set gives a much higher D than experiment, but predicts negligible contribution from C_3H_6O and O_2. Product species and molar concentrations from the T-Jump experiments are compared with CHEETAH calculations in Table 1.

Explosive Power and Air Blast Energy

Data for explosive power and sensitivity of TATP and HMTD were collected from several sources [6, 10-13] and compared to common primary and secondary explosives in Table 2. The peroxide compounds have a higher explosive power than traditional primary explosives, but are also much more sensitive.

Table 2.   Explosive power and sensitivity for peroxides and other common explosives

Explosive	Explosive Power (% TNT)			Sensitivity	
	ΔH_d Ratio	Trauzl Test	Sand Crush Test	Impact (N-m)	Friction (N)
TATP	61	83-88	83	0.3	<0.1
HMTD	92	60-110	103[a]	0.6	<0.1
Mercury fulminate	38-43	37-51	50-55	1-2	3-5
Lead azide	33-36	37-40	40-45	2.5-4[b]	0.1-1
PETN	129-139	174	131-141	3	60
RDX	113-139	158-161	123-129	7.5	120
TNT	100	100	100	15	>353

[a] Sand crush test used 50 g instead of standard 40 g of explosive.
[b] Values for non-dextrinated lead azide.

JWL parameters (eq. 1) were calculated in CHEETAH and used in AUTODYN air blast models. Parameter are for HMTD using the default product set (A = 73.24 GPa, B = 1.33 GPa, R_1 = 4.70, R_2 = 1.02, ω = 0.31, D_{CJ} = 4.34 m/ms, E_0 = 3.12 kJ/cc, P_{CJ} = 4.25 GPa) and TATP using the T-Jump product set (A = 24.62 GPa, B = 0.63 GPa, R_1 = 4.93, R_2 = 0.94, ω = 0.15, D_{CJ} = 3.16 m/ms, E_0 = 3.608 kJ/cc, P_{CJ} = 1.95 GPa). TNT equivalence (TNT_{eq}) values were calculated using the incident blast pressure (P_{so}) and impulse (I_{so}) from 1-kg spherical charges. There were only slight variations in the TNT_{eq} values over a scaled distance of Z = 2-5 m/kg$^{1/3}$. The averaged TNT_{eq} from P_{so} and I_{so} over this range were equivalent giving values of TNT_{eq} = 0.92 for TATP and TNT_{eq} = 0.82 for HMTD. These TNT_{eq} values are similar to those predicted using

the CHEETAH energy of detonation. However, they differ from the explosive power trends seen in the literature data (Table 2), where HMTD is the more powerful peroxide.

Non-Ideal IEM Modelling

Detonation Velocity (Size Effect)

Size or diameter effect (SE) data, i.e. the change in steady state detonation velocity with radius for cylinders, has been collected from literature [14-18] for several common improvised explosives and fit to the Campbell-Engelke [19] relation,

$$D(R_o) = D_\infty \left[1 - \frac{A}{(R_o - R_c)} \right].$$ (10)

R_o is the charge radius, A and R_c are constants, and D_∞ is the infinite radius detonation velocity obtained by plotting detonation velocity vs. inverse radius and extrapolating to zero. SE curves for several IEM are shown in Figure 2.
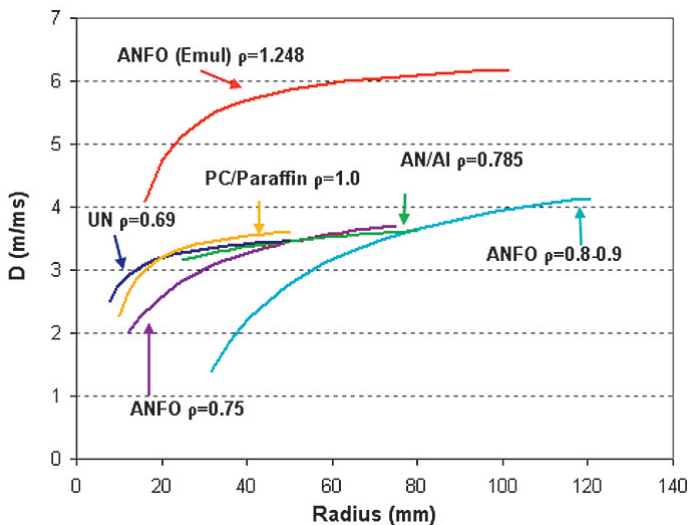
Figure 2. Curve-fit size effect data from literature for several IEM.

ANFO prill ($\rho = 0.8$-0.9) is commonly used for commercial blasting and has more SE data available than other IEM. SE data for ANFO $\rho = 0.75$

comes from experiments using ground ammonium nitrate (AN), and exhibits a lower failure diameter and D_∞. ANFO used in these experiments was 94% AN and 6% fuel oil by weight. ANFO emulsion consists of (by wt.) 77% AN, 16% water, 6% mineral oil, and 1% emulsifier which is then mixed with 1% microballoons to obtain $\rho = 1.248$. ANFO emulsion is not a common IEM, but is included for additional model validation. The AN/Al composition is 82% AN and 18% aluminum (spherical, average particle size 10.5 μm). The curve for PC/Paraffin $\rho = 1.0$ was calculated with I&G models using paper confinement data [20]. Campbell-Engelke fit constants for the IEM modelled are given in Table 3.

Table 3.   Campbell-Engelke parameters for the non-ideal IEM investigated

| Explosive	Ref.	ρ (g/cm³)	$D\infty$ (m/ms)	A (mm)	R_c (mm)
ANFO (all)	[14-16]	0.8-0.9	5.10	22.57	0.41
ANFO (Emul.)	[18]	1.248	6.45	4.10	4.73
UN	[16]	0.69	3.63	2.395	0
PC/Paraffin	This work (Calc.)	1.0	3.82	2.66	3.48

The ANFO EOS parameters (JWL and unreacted) were taken from literature [14]. JWL parameters for all other explosives were determined using CHEETAH calculations and adjusted to fit experimental D_∞. Unreacted EOS parameters for ANFO emulsion ($\rho = 1.248$) were available in literature [21], while UN and PC/Paraffin assumed values based on $C_0 \approx 10\%$ of the solid (ρ_{TMD}) material and $s \approx 2$.

Souers proposed an edge of convergence of 8 zones across the effective reaction zone, $<x_e>$, for I&G models [22]. From literature, the minimum $<x_e>$ for ANFO $\rho = 0.8$ and ANFO $\rho = 1.248$ were 10 mm and 8 mm respectively [18]. Convergence was achieved with 1.0 mm cells for ANFO ($\rho = 0.8$ and $\rho = 1.248$) and 0.5 mm for UN and PC/Paraffin. Models using twice these cell sizes (2.0 mm and 1.0 mm) gave similar results.

I&G and K-CHEETAH models were fitted to the SE data by adjusting G and b in the reaction rate equation (eq. 3). Souers *et al.* [2] found that changing b adjusts the SE plot curvature as observed with the ANFO models in Figure 3a. A value of $b = 1.0$ gave a reasonable fit for ANFO, UN, and PC/Paraffin I&G models and was assumed for *all* K-CHEETAH reactants. "Unconfined" experimental SE data usually have some light confinement such as paper tubes or PVC pipe. The difference between I&G model SE curves for unconfined or PVC confined

rate sticks is shown for UN in Figure 3b. The K-CHEETAH calculations for UN assumed radius of curvature values from PVC confined I&G models.
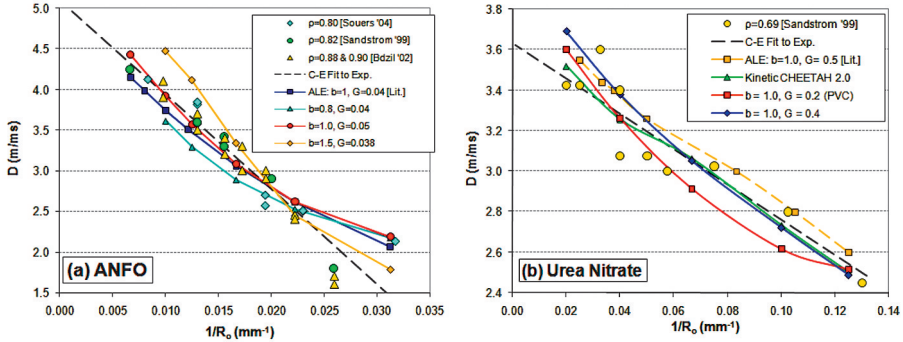

Figure 3. Experimental SE data and models for (a) ANFO and (b) UN. Values of G and b obtained for unconfined ANFO and UN are similar to those reported in literature for the ALE code [14, 23, 24].

As R_o increases, detonation velocity in some of the I&G models appears to be approaching a D_∞ that is larger than the experimental values. K-CHEETAH models converge to the calculated D_{CJ}, which may be different than D_∞ from SE data. To overcome this, the UN (shown in Figure 3b) used the BKWC product library for K-CHEETAH so that $D_{CJ} \approx D_\infty$. At smaller radii the ANFO I&G models differ from experiment and it has been noted in literature that simple I&G models (e.g. JWL++) are not able to correctly predict detonation failure [17, 22].

Detonation Front Curvature and the Reaction Zone

I&G reactive flow models were successful in reproducing the reaction zone and front curvature. Paper confinement ($\rho = 0.683$) has little effect on the curvature, but decreased curvature and edge lag is observed with PVC and steel confinement. Experimental curvature measurements for UN [16], ANFO [16], and ANFO emulsion [18] where PVC ("plastic") confinement was used agree well with PVC confined I&G models.
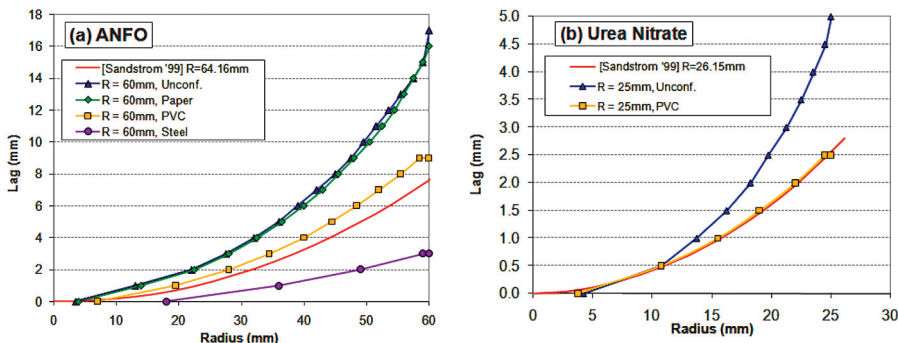
Figure 4.   Experimental and calculated shock front curvatures for (a) ANFO
and (b) UN.

The reaction zone lengths were calculated as the distance from the shock
front to the sonic plane, which is found in the I&G models from [2, 25]:

$$\left(U_{p,x}^2 + U_{p,y}^2\right)^{1/2} + c = U_s . \tag{11}$$
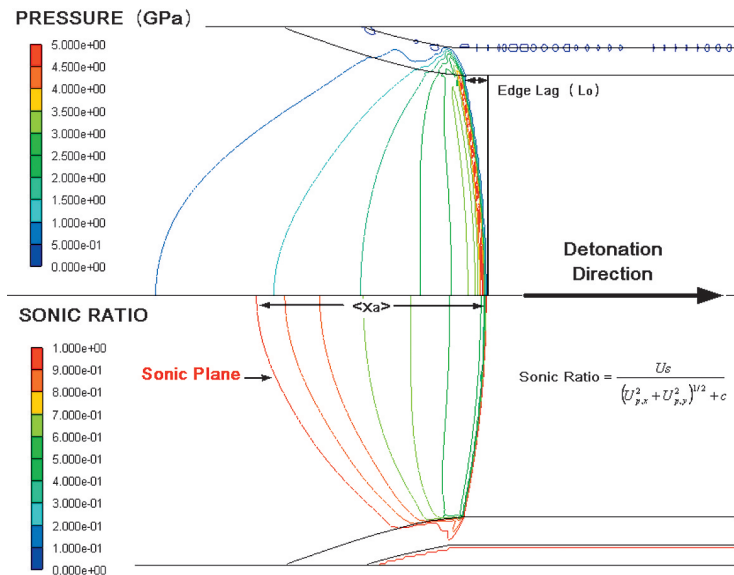
Figure 5.   Pressure and sonic ratio countours for R=50 mm UN in PVC.

Obtained I&G reaction zones were much larger than the edge lag, L_o, and
increased with R_o and confinement. Figure 5 shows contour plots from I&G for

pressure and a sonic ratio based on eq. 11. Energy released after the sonic plane does not support the shock front, but can contribute to the overall detonation energy.

Expansion and Detonation Energy

Expansion of the detonation products for ANFO is shown using pressure-volume (P-V) plots in Figure 6 for I&G and K-CHEETAH models. As the charge radius increases, the detonation pressure and energy are expected to approach an infinite radius (R_∞) scenario. This is represented by the CJ theory JWL isentrope for K-CHEETAH and the Program Burn model in AUTODYN. While the K-CHEETAH results exhibit this convergence to R_∞ values, the I&G models do not, which is partially due to the pressure equilibrium between the reacted and unreacted explosive required by the Lee-Tarver solver. Expansion in the K-CHEETAH models starts at the steady state detonation point and is coincident to the Rayleigh line. In the I&G models the Rayleigh line is well below the spike point, but approaches the P-V point at the back of the shock front (which is the jump observed at $V \approx 0.75$). The sonic points calculated from eq. 11 show that the back of the reaction zone in the I&G models occurs at a much larger expansion than K-CHEETAH.
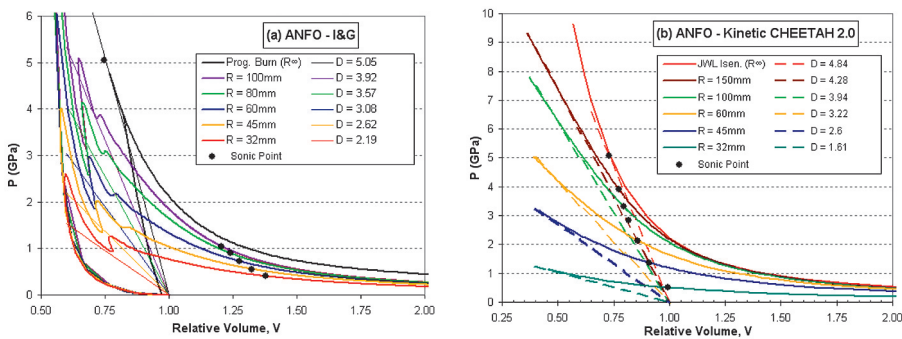
**Figure 6.**   P-V plots for ANFO from (a) I&G models and (b) K-CHEETAH.

Detonation energies shown in Figure 7 are calculated from eq. 9 for I&G and eq. 8 for K-CHEETAH models. The negative values of detonation energy during shock compression are not shown. In both cases, E_{det} increases with radius to a maximum value (which coincides with complete burn, $F \approx 1.0$) and then decreases slightly with additional increase in radius. In the K-CHEETAH models E_{det} converges to the JWL isentrope, but for I&G the maximum E_{det} is substantially less than the isentrope and shows little increase after $V \approx 5$.
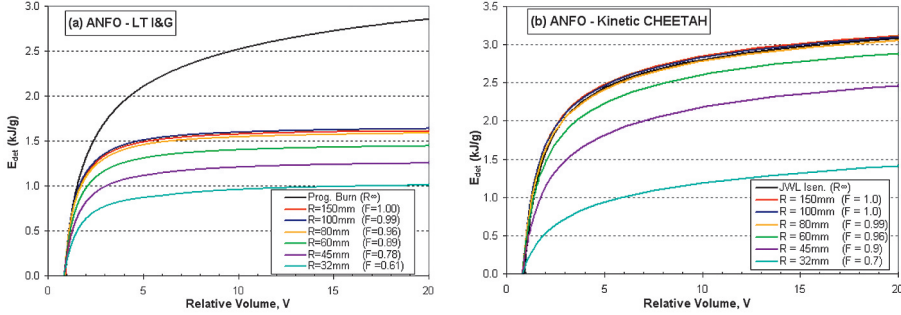
Figure 7.   Detonation energy for ANFO from (a) I&G models and (b) K-CHEETAH.

It was proposed that the burn fraction at the back of the reaction zone, F_e, can be related to other detonation parameters through [6],

$$F_e \approx \frac{E_0}{E_D} \approx \frac{P_M}{P_D} \approx \left(\frac{U_s}{D}\right)^2. \tag{12}$$
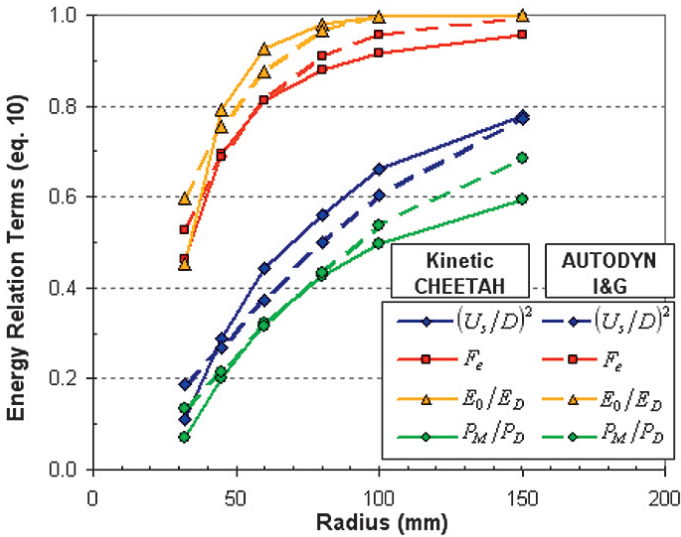
Figure 8.   Energy relations for unconfined ANFO models.

E_0, P_M, and U_s are the total detonation energy, maximum pressure, and detonation velocity for radius R_o and E_D, P_D, and D are the corresponding variables

at infinite radius, R_∞. I&G and K-CHEETAH show comparable trends with E_0/E_D and F_e being similar but larger than the $(U_s/D)^2$ and P_M/P_D quantities (Figure 8). E_D values for the I&G models were taken from the $R_o = 150$ mm model.

Confinement Effects

Figure 9 gives some results of ANFO confinement in paper, PVC, and steel with I&G models. A Linear $(U_s\text{-}u_p)$ EOS (eq. 6) was used for confinement materials. EOS parameters for PVC ($\rho = 1.376$ g/cm³, $C_0 = 2.314$ m/ms, $s = 1.469$) were estimated from Hugoniot data [26]. Paper assumed $\rho = 0.683$ g/cm³ [17] and values were interpolated from data for low density wood ($C_0 = 0.66$ m/ms, $s = 1.43$) [26]. Steel values are from the AUTODYN material library. Wall thicknesses were based on commercial "Schedule 40" pipe for PVC and steel. Paper confined ANFO models had a thickness of 6 mm to match experiments [15].
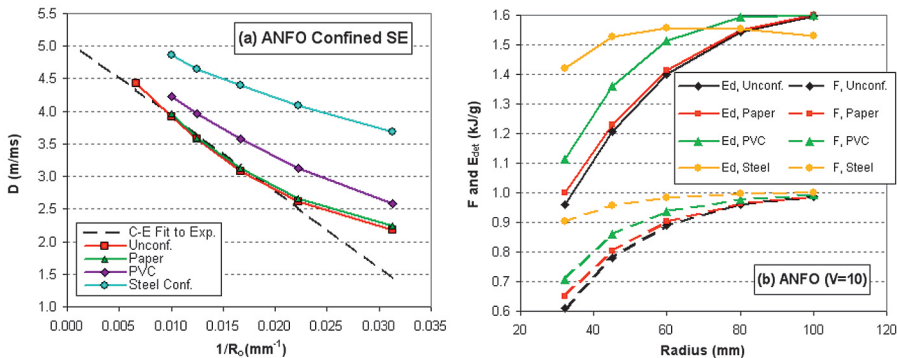

Figure 9.　Effect of confinement on (a) the SE curves and (b) E_{det} and Reaction Ratio (F) for ANFO I&G models (all using $G = 0.05G$ pa⁻¹μs⁻¹, $b = 1.0$).

D, F, and E_{det} increase with confinement density, but there was some saturation observed in E_{det} for steel confinement. Some models with steel and copper confinement (larger C_0 and ρ) had shocks which travel ahead of the detonation front through the wall and can cause premature ignition of the explosive.

Air Blast Energy

The energy release from the K-CHEETAH models (shown earlier) is a more accurate representation of the non-ideal detonation process than the I&G models. Therefore, initial air blast models use a Program Burn method with JWL parameters fitted to the K-CHEETAH P-V curves for each ANFO

charge radius (Figure 6b). Cylindrical charges of L/D = 4.0 were modelled in AUTODYN with gauges located at 90º from the charge axis at scaled distances of Z = 1.0 to 5.0 m/kg$^{1/3}$. This location coincides with the area of peak pressure and impulse for the cylindrical charge geometry. Ratios of the incident blast pressure, P_{so}, and impulse, I_{so}, for each charge radius to a blast model using the infinite radius JWL were calculated. These ratios, shown in Figure 10, indicate that assuming ideal behaviour may be a significant overestimate for smaller charges and standoff distances.
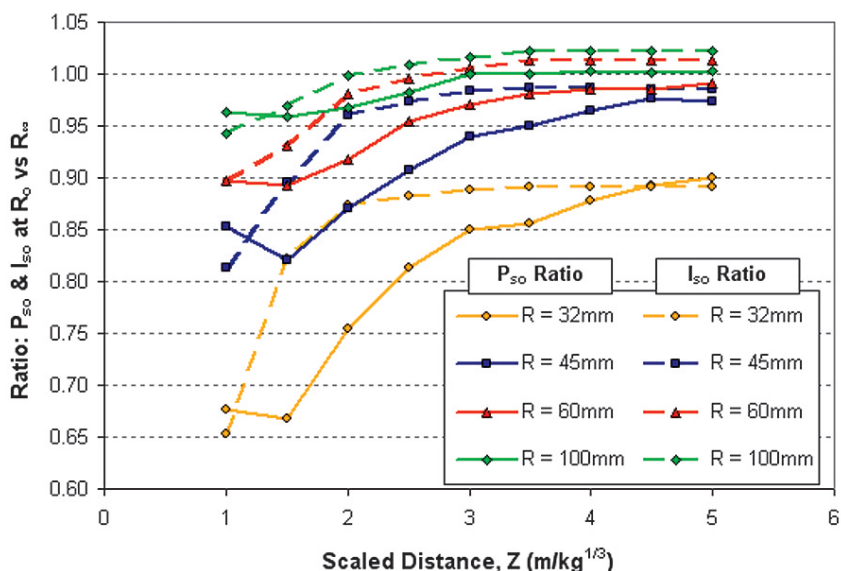
Figure 10. Ratio of P_{so} and I_{so} at varius ANFO radii (R_o) to R_∞ for air blast models using K-CHEETAH fitted JWLs.

Conclusions

CHEETAH 2.0 calculations along with AUTODYN air blast and reactive flow models have shown success in calculating the detonation velocity and energy for peroxide and non-ideal IEM. Detonation velocities for TATP and HMTD predicted with CJ theory show agreement to literature. For TATP, CHEETAH calculations using a limited product set based on T-Jump experimental results in literature gives a better prediction of the detonation velocity at bulk density. TNT equivalency was calculated from air blast models as 0.92 for TATP and 0.82 for HMTD.

The Kinetic CHEETAH and I&G methods for modeling non-ideal explosives have advantages and limitations. Kinetic CHEETAH can be quickly calibrated to the SE data and predict the steady detonation condition, sonic point, and detonation energy but the calculations require input for the radial expansion terms or radius of curvature. Reactive flow models using the Lee-Tarver I&G method with a single growth term can simulate the detonation behavior for confined charges and give shock front curvatures which closely match experimental data when the confinement conditions are modeled. However, the pressure equilibrium method used in the Lee-Tarver solver can be computationally demanding and results in a rapid decrease in detonation pressure following the shock front. Consequently, the detonation energies are lower than expected and do not converge (with increasing radii) to the JWL isentrope calculated from CJ-theory. AUTODYN air blast models for ANFO using JWL parameters fitted to K-CHEETAH calculations show that considering the non-ideal effects on energy release is important for smaller radii charges and shorter standoff distances ($< Z \approx 4$ m/kg$^{1/3}$).

References

[1] Fried L.E., Howard W.M., Souers P.C., *CHEETAH 2.0 User's Manual*, Lawrence Livermore National Laboratory Report, UCRL-MA-117541, Rev. 5, **1998**.

[2] Souers P.C., Anderson S., Mercer J., Mcguire E., Vitello P., JWL++, A Simple Reactive Flow Code Package for Detonation*, Propellants, Explos., Pyrotech.*, **2000**, *25,* 54-58.

[3] Wescott B.L., Generalized Pseudo-Reaction Zone Model for Non-Ideal Explosives, *Shock Comp. Cond. Mat.*, **2007**, *955,* 433-436.

[4] Davis L.L., Hill L.G., ANFO Cylinder Tests*, Shock Comp. Cond. Matt*., **2001***, 620*, 165-168.

[5] Kuzmin V.V., Kozak G.D., Solov'ev M., Tuzkov Y.B., Forensic Investigation of Some Peroxides Explosives, *New Trends in Research of Energetic Materials,* Czech Republic, April 09-11, **2008**, 386-392.

[6] Federoff B.T., *Encyclopedia of Explosives and Related Items*, Volumes 1-10, Picatinny Arsenal, Dover, New Jersey, USA, **1960-1983**.

[7] Dubnikova F., Kosloff R., Almog J., Zeiri Y., Boese R., Itzhaky H., Alt A., Keinan E., Decomposition of Triacetone Triperoxide is an Entropic Explosion*, J. Amer. Chem. Soc*., **2005**, *127,* 1146-1159.

[8] Hiyoshi R.I., Nakamura J., Brill T.B., Thermal Decomposition of Organic Peroxides TATP and HMDT by T-Jump/FTIR Spectroscopy, *Propellants, Explos., Pyrotech.,* **2007**, *32*(2), 127-134.

[9] ICT: ICT Database of Thermochemical Values, version 5, **2003**.

[10] Meyer R., Kohler J., Holmberg A., *Explosives*, 5th ed., Wiley-VCH, Verlag GmbH, **2002**.

[11] Dobratz B.M., Crawford P.C., *LLNL Explosives Handbook*, Lawrence Livermore National Laboratory, California, UCRL-52997, **1985**.

[12] Akhavan J., *The Chemistry of Explosives,* RSC Paperbacks, The Royal Society of Chemistry, **1998**.

[13] Cooper P.W., Comments on TNT equivalence*, 20th International Pyrotechnics Seminar*, Colorado Springs, CO, July 24-29, **1994**.

[14] Souers P.C., Vitello P., *ANFO Calculations for Sedat Ensen*. LLNL, UCRL-TR-204259. May 20, **2004**.

[15] Bdzil J.B., Aslam T.D., Short M., DSD Front Models, Nonideal Explosive Detonation in ANFO, *Proc. 12th Int. Symp. Det.*, San Diego, California, Aug. 11-26, **2002**.

[16] Sandstrom F.W., Abernathy R.L. et al., Diameter Effect and Detonation Front Curvature of Ideal and Non-Ideal Explosives*. Shock Compression of Condensed Matter*, **1999**, *505*, 825-828.

[17] James H.R., Lambourn B.D. et al., An Investigation of the Detonation Characteristics of Some Non-Ideal Explosive Compositions Based Upon Ammonium Nitrate, *Proc. 13th Int. Symp. Det.*, Norfolk, Virginia, July 23-28, **2006**.

[18] Souers P.C., Wu B., Haselman L.C., Jr., *Detonation Equation of State at LLNL, 1995,* Lawrence Livermore National Laboratory, UCRL-TD-119262, Feb. 1, **1996**.

[19] Campbell W., Engelke R., The Diameter Effect in High-Density Heterogeneous Explosives, *Proc. 6th Int. Det. Symp.*, Coronado, California, Aug. 24-27, **1976**, 642-652.

[20] Davis T.L., *The Chemistry of Powder and Explosives,* Angriff Press, Hollywood, CA. **1941**, **1943** (reprint of two volumes).

[21] Lee J., Sandstrom F.W., Craig B.G. Persson P.-A., Detonation and Shock Initiation Properties of Emulsion Explosives, *Proc. 9th Int. Symp. Det.*, Portland, OR, Aug. 28-Sept. 1, **1989**, 573-583.

[22] Souers P.C., Garza R., Vitello P., Ignition & Growth and JWL++ Detonation Models In Coarse Zones*, Propellants, Explos., Pyrotech.,* **2002**, *27*, 62-71.

[23] Souers P.C., Anderson S., Mcguire E., Murphy M.J., Vitello P., Reactive Flow and the Size Effect, *ibid.*, **2001***, 26*, 26-32.

[24] Howard W.M., Fried L.E., Souers P.C., Vitello P.A., Calculation of Chemical Detonaion Waves with Hydrodynamics and Thermochemical Equation of State, *Shock Compression of Condensed Matter - 2001*, *12th APS Topical Conference*, **2001**, *620*, 161-164,

[25] *LASL Shock Hugoniot Data*, (Marsh S.P., Ed.), Univ. Of Calif. Press, Berkley, California **1980**.

[26] Souers P.C., Vitello P., Analytical Model of Reactive Flo*w, Propellants, Explos., Pyrotech.*, **2005**, *32*(5), 381-385.